Molecular Therapy
Nucleic Acids
Original Article

Cannabinoid Receptor 1/miR-30b-5p Axis Governs Macrophage NLRP3 Expression and Inflammasome Activation in Liver Inflammatory Disease

Le Yang,[1,3] Lei Tian,[1,3] Zhi Zhang,[1,3] Xuan Zhou,[1] Xiaofang Ji,[1] Fuquan Liu,[2] Chengbin Dong,[2] Lei Hou,[1] Xinhao Zhao,[1] Na Chang,[1] Lin Yang,[1] and Liying Li[1]

[1]Department of Cell Biology, Municipal Laboratory for Liver Protection and Regulation of Regeneration, Capital Medical University, Beijing 100069, China; [2]Department of Interventional Therapy, Beijing Shijitan Hospital, Capital Medical University, Beijing 100069, China

Nod-like receptor (NLR) family pyrin domain containing 3 (NLRP3) has been regarded as an important initiator or promoter in multiple inflammatory diseases. However, the relationship between cannabinoid receptor 1 (CB1) and macrophage NLRP3 inflammasome and the corresponding molecular mechanism in liver inflammation remain unclear. Mouse liver injury models were induced by carbon tetrachloride (CCl_4) or methionine-choline-deficient and high fat (MCDHF) diet. Human liver tissues were obtained from patients with different chronic liver diseases. CB1 expression was increased in liver tissue and macrophages of CCl_4- and MCDHF-treated mice, positively correlated with NLRP3. CB1 agonist ACEA (Arachiodonyl-2'-Chloroethylamide) promoted NLRP3 expression and NLRP3 inflammasome activation in macrophages. CB1 blockade with its antagonist AM281 reduced NLRP3 expression, inflammasome activation, and liver inflammation in CCl_4- and MCDHF-treated mice. MicroRNA-30b-5p (miR-30b-5p), screened by the intersection of bioinformatics databases and downregulated miRNAs in injured liver, negatively correlated with NLRP3 in mouse and human liver. miR-30b-5p was involved in CB1-mediated activation of NLRP3 inflammasome in macrophages by directly targeting NLRP3. Importantly, administration of miR-30b-5p agomir targeted NLRP3 and attenuated liver inflammation in the injured liver. Altogether, CB1/miR-30b-5p axis modulates NLRP3 expression and NLPR3 inflammasome activation in macrophages during liver inflammation, which provides a potential target for liver disease.

INTRODUCTION

Inflammasomes are protein complexes that serve as pattern recognition receptors and intersect with a wide variety of immune pathways.[1–3] Nod-like receptor (NLR) family pyrin domain containing 3 (NLRP3), the most well studied inflammasome, belongs to NLR family and forms a complex comprising adaptor proteins, such as apoptosis-associated speck-like protein (ASC) and the serine protease caspase-1. NLRP3 inflammasome activation governs the cleavage and activation of caspase-1, leading to maturation of effector pro-inflammatory cytokines, such as pro-interleukin (IL)-1β and pro-IL-18.[4–7] Aberrant activation of NLRP3 inflammasome has been regarded as an important initiator or promoter in multiple diseases, such as autoimmune disease, cancer, neurodegenerative disorders, and so on.[8–11] For instance, NLRP3 inflammasome activation was increased in the adipose tissue and liver of obese mice and humans, and its expression level was directly correlated with the severity of type 2 diabetes in obese individuals.[12] Notably, myeloid-specific NLRP3 inflammasome hyperactivation resulted in predominant neutrophilic infiltration and hepatic stellate cell activation, leading to severe liver inflammation and fibrosis in mice.[13] Although the critical role of NLRP3 inflammasome has been identified in various pathological conditions of liver disease, the precise epigenetic regulation of NLRP3 inflammasome in macrophages during liver injury remains incompletely understood.

MicroRNA (miRNA), a sort of single-stranded noncoding small RNA, is known to negatively regulate gene expression posttranscriptionally, either by inhibiting translation or destabilizing its target transcripts.[14–16] Recent studies have identified that NLRP3 can be regulated by several miRNAs in various diseases, including miR-22-3p,[17] miR-21,[18] miR-132,[19] miR-181a,[20] and so on. However, few studies have investigated which miRNAs might target and regulate NLRP3 in macrophages during liver injury. Since the expression pattern of miRNAs is tissue- and cell-specific, it is worthwhile to further explore the regulative effect of miRNAs on the expression and activation of NLRP3 inflammasome in macrophage-associated liver inflammation.

Received 7 April 2020; accepted 22 April 2020;
https://doi.org/10.1016/j.omtn.2020.04.010.

[3]These authors contributed equally to this work.

Correspondence: Liying Li, Department of Cell Biology, Municipal Laboratory for Liver Protection and Regulation of Regeneration, Capital Medical University, Beijing 100069, China.
E-mail: liliying@ccmu.edu.cn

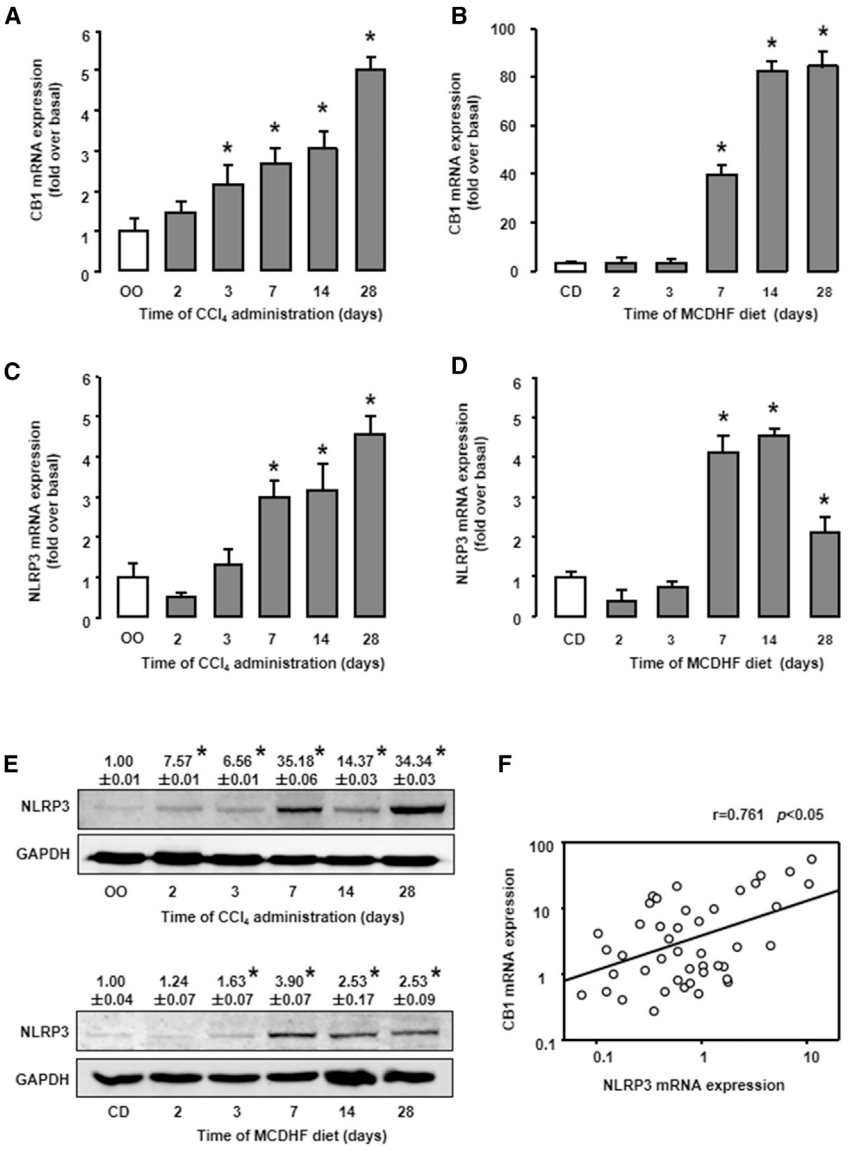

Figure 1. The NLRP3 Expression in Injured Liver and the Correlation between NLRP3 and CB1 Expression in Liver

(A) CB1 mRNA expression in the fibrotic liver of CCl_4 mice. (B) CB1 mRNA expression in the fibrotic liver of MCDHF mice. (C) NLRP3 mRNA expression was examined by qRT-PCR in the fibrotic liver of CCl_4 mice. (D) NLRP3 mRNA expression in the fibrotic liver of MCDHF mice. (E) NLRP3 protein expression was examined by western blot in the fibrotic liver of CCl_4 and MCDHF mice. (F) The correlation between CB1 and NLRP3 mRNA expression in liver tissue. Data are presented as the mean ± SEM. n = 6 per group. *p < 0.05 versus control. OO, olive oil; CCl_4, carbon tetrachloride; CD, control diet; MCDHF, methionine-choline-deficient and high fat.

The endocannabinoid system (ECS) has been shown to regulate a variety of biological processes, including memory, appetite, energy metabolism, and immunity.[21,22] Endocannabinoids (anandamide, AEA; 2-arachidonoylglycerol, 2-AG) are endogenous lipid ligands, which can bind to two G protein-coupled cannabinoid receptors (CB1 and CB2) and trigger a cascade of intracellular signal activation, leading to specific gene expression and various cellular responses, including inflammation and tissue repair.[23] For example, CB1 contributed to lipopolysaccharide-induced inflammation and insulin resistance in the model of metabolic endotoxemia.[24] An imbalance in the renal ECS with CB1 signaling prevailing over that of CB2, resulted in oxidative stress and inflammation followed by cell dysfunction, apoptosis, and kidney fibrosis.[25] As for the role of ECS in liver, CB1 promoted hepatocellular carcinoma initiation and progression by the induction of various tumor-promoting genes.[26] CB2 activation decreased liver inflammation and fibrosis by reducing IL-17 production by T helper 17 (Th17) lymphocytes via a STAT5-dependent pathway and by blunting the pro-inflammatory effects of IL-17 on its target cells, while preserving IL-22 production.[23] Our previous studies had also found that CB1 promoted the infiltration and activation of monocytes/macrophages in liver injury mouse model.[27–29] Nevertheless, the relationship between CB activation and NLRP3 inflammasome and the corresponding molecular mechanism in macrophages during liver inflammation and injury has not yet been well demonstrated.

The current study uncovers a critical role of CB1 in macrophage NLRP3 inflammasome and identifies miR-30b-5p as a negative regulator of NLRP3 expression and NLRP3 inflammasome activation in macrophages during liver inflammation and injury. These data expand our understanding of NLRP3 inflammasome in liver inflammation and indicate that CB1/miR-30b-5p-based therapies are anticipated for treatment of liver disease.

RESULTS

CB1 Expression Was Increased in Injured Liver and Positively Correlated with NLRP3

We first examined the expression of CB1 in chronic liver injury in mice. We used two mouse models of liver injury induced by carbon tetrachloride (CCl_4) or feeding a methionine-choline-deficient and high fat (MCDHF) diet. The result of qRT-PCR showed that CB1 mRNA expression was significantly increased at day 3 of CCl_4 administration, continued to increase as the administration time prolonged, and peaked at 4 weeks (Figure 1A). Similar results were detected in the liver of MCDHF mice. The mRNA expression of CB1 began to increase at day 7 of MCDHF diet and continuously

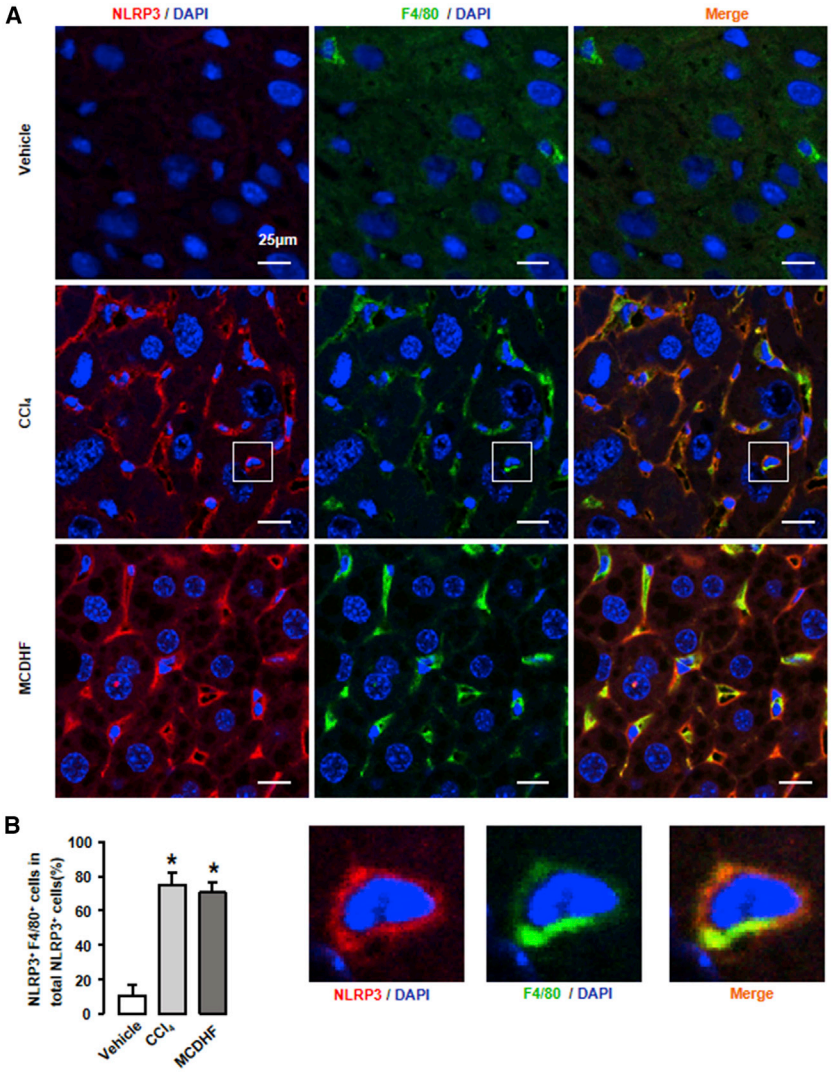

Figure 2. The NLRP3 Expression in Macrophages of Injured Liver

(A) Representative images of immunofluorescence analysis of NLRP3 (red) and F4/80 (green) expression in the fibrotic liver. (B) The proportion of $NLRP3^+/F4/80^+$ cells accounting for total $NLRP3^+$ cells was measured by Image-Pro Plus software. Data are presented as the mean ± SEM. n= 6 per group. *$p < 0.05$ versus control. CCl_4, carbon tetrachloride; MCDHF, methionine-choline-deficient and high fat.

increased throughout the entire stage of chronic liver injury, reaching its peak around 2 weeks (Figure 1B). Then we examined NLRP3 expression in the injured liver, showing the significant upregulation of NLRP3 mRNA expression in the damaged liver of CCl_4 (Figure 1C) and MCDHF mice (Figure 1D). Meanwhile, we detected the expression of NLRP3 at the protein levels in the injured liver. As shown in Figure 1E, western blot analysis revealed a pronounced increase in hepatic NLRP3 expression after CCl_4 treatment and MCDHF diet feeding. We then undertook correlation analysis of mRNA expression levels between CB1 and NLRP3. Each dot represented one liver sample from all mice (including OO-, CCl_4-, CD-, and MCDHF-treated groups). Correlation coefficients were calculated using relative mRNA expression levels of CB1 and NLRP3 from the same sample by Pearson correlation test. The result showed that there was a positive correlation between the expression of CB1 and NLRP3 in liver (Figure 1F), indicating that CB1 might be involved in NLRP3 inflammasome activation. Altogether, these results showed that CB1 expression was upregulated in the injured liver of CCl_4 and MCDHF mice, and CB1 might play a potential role in the regulation of NLRP3 expression during liver injury.

NLRP3 Was Expressed in Macrophages of Injured Liver, Positively Correlated with CB1 Expression in Macrophages

Although NLRP3 was expressed in a variety of cells, a large body of literature indicated that NLRP3 inflammasome in macrophage played an important role in the development and progression of disease.[30] Next we verified whether NLRP3 was expressed in the macrophages of injured liver. Immunofluorescence staining showed that there was low expression of NLRP3 in the liver of control group, while NLRP3 expression was found to be significantly increased in CCl_4- and MCDHF-induced mouse injured liver (Figures 2A and 2B). In addition, we quantified the proportion of both F4/80 (macrophage marker)-positive and NLRP3-positive cells among total NLRP3-positive cells using the software Image-Pro Plus. Our result showed that NLRP3 was mainly expressed in macrophages, as demonstrated by the fact that percentage of $NLRP3^+/F4/80^+$ cells accounting for total $NLRP3^+$ cells was more than 70% (Figure 2B).

To confirm the role of NLRP3 on macrophages *in vivo*, we isolated liver macrophages from non-parenchymal cells of mouse liver as published previously[27] and identified them by fluorescence-activated cell sorting (FACS) analysis of F4/80 expression (Figure 3A). We then detected the mRNA expression levels of CB1 and NLRP3 in isolated liver macrophages after 4 weeks of CCl_4 administration or 2 weeks after MCDHF diet. qRT-PCR results showed a significant increase in both CB1 (Figure 3B) and NLRP3 (Figure 3C) expression in the injured liver. We also analyzed the correlation between CB1 and NLRP3 mRNA expression using linear correlation analysis, finding that the expression of CB1 in macrophages was positively correlated with the expression of NLRP3 (Figure 3D). Collectively, these results indicated that NLRP3 was mainly expressed in macrophages of injured liver

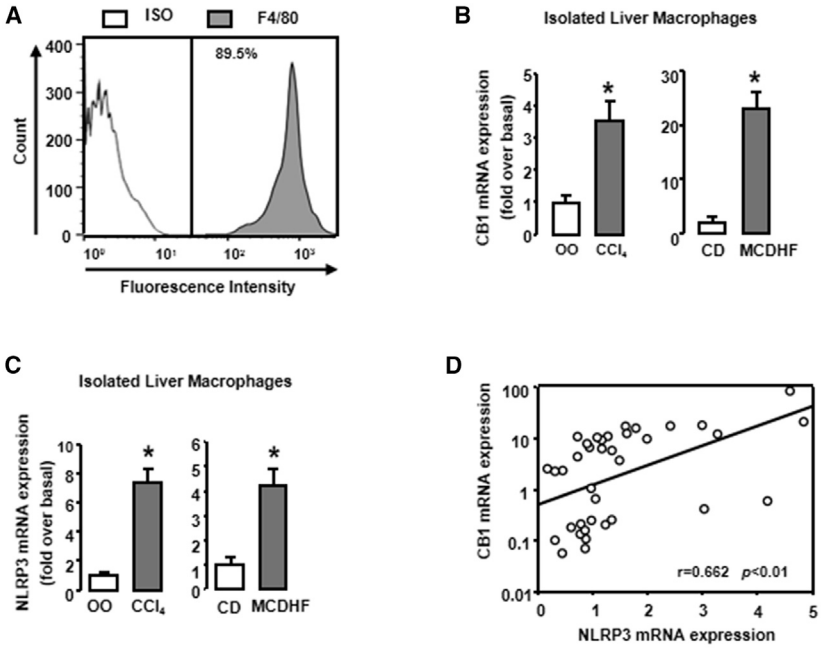

Figure 3. The NLRP3 Expression in Isolated Liver Macrophages and the Correlation between NLRP3 and CB1 Expression in Macrophages

(A) Representative FACS histograms and plots for F4/80 expression. (B) CB1 mRNA expression in the isolated liver macrophages of CCl_4 and MCDHF mice was examined by qRT-PCR. (C) NLRP3 mRNA expression in the isolated liver macrophages of CCl_4 and MCDHF mice. (D) The correlation between CB1 and NLRP3 mRNA expression in the isolated liver macrophages. Data are presented as the mean ± SEM. n = 6 per group. *p < 0.05 versus control. OO, olive oil; CCl_4, carbon tetrachloride; CD, control diet; MCDHF, methionine-choline-deficient and high fat.

and CB1 was involved in the regulation of NLRP3 inflammasome in macrophages.

CB1 Activation Promoted NLRP3 Expression in Macrophages

Large numbers of bone marrow-derived monocyte/macrophages (BMMs) were recruited to the injured liver and played an important role in liver inflammation and injury in mice.[27,28] To demonstrate the effect of CB1 on NLRP3 expression in macrophages *in vitro*, we stimulated cultured BMMs with CB1 agonist ACEA for 6 h and detected the NLRP3 mRNA expression levels. qRT-PCR results showed that ACEA (1 μmol/L) promoted the mRNA expression levels of NLRP3 at 6 h (Figure 4A), implying that the activation of CB1 effectively promoted NLRP3 expression. When BMMs were pretreated with AM281 (CB1 antagonist), ACEA-induced elevations of NLRP3 mRNA levels were suppressed (Figure 4A). To confirm the critical role of CB1, we employed CB1-specific small interfering RNA (siRNA) and measured the silencing efficiency of CB1 siRNA at mRNA level. After transfection of BMMs with CB1 siRNA, the mRNA expression of CB1 was reduced to 43% (Figure 4B), which was in accordance with the experimental requirements. Similar to the AM281 pretreatment results, silencing CB1 expression with siRNA abrogated the enhancement of NLRP3 expression induced by ACEA in BMMs (Figure 4C). Collectively, these results indicated that CB1 activation promoted the expression of NLRP3 in macrophages.

CB1 Blockade Reduced NLRP3 Expression, Activation of NLRP3 Inflammasome, and Liver Inflammation *In Vivo*

To confirm the pivotal role of CB1 in the regulation of NLRP3 expression in insulted liver, we performed administration of CB1 antagonist, AM281, in the mouse models. As expected, AM281 injection markedly reduced the mRNA levels of NLRP3 in injured livers of CCl_4-treated mice compared with that in CCl_4-treated alone (Figure 5A). Similar to the result of CCl_4-induced murine liver injury, AM281 pre-treatment also reduced the mRNA expression of NLRP3 in the damaged liver of MDCHF mice (Figure 5B). Consistent with the mRNA results, AM281 pretreatment reduced the expression of NLRP3 protein levels in the injured liver (Figure 5C). Furthermore, we investigated the changes of NLRP3 inflammasome activation product IL-1β and measured the protein levels of IL-1β in liver using CBA kit (Figure 5D). AM281 administration significantly decreased the protein levels of IL-1β in the injured liver of CCl_4 (Figure 5E) and MCDHF mice (Figure 5F). Hematoxylin & eosin (H&E) staining showed a significant decrease in liver inflammation and injury after the administration of AM281 (Figure 9A) and the area of inflammation quantified by digital image analysis was dramatically reduced with AM281 injection in MCDHF mice (Figure 9B). The results verified that CB1 blockade *in vivo* resulted in the suppression of NLRP3 expression, activation of NLRP3 inflammasome, and the attenuation of liver inflammation.

miR-30b-5p Targeting NLRP3 Was Screened by the Intersection of Bioinformatics Databases and Downregulated miRNAs in the Injured Liver of Mouse and Human

In recent years, a large number of studies have shown that miRNA can regulate the expression of most genes at the transcriptional level and affect the function of cells.[31] Therefore, we next sought to investigate whether one or some miRNAs were involved in the regulation of NLRP3 mRNA expression by CB1. To identify the miRNAs targeting NLRP3, we intersected the predicted miRNAs from two databases (http://www.targetscan.org; http://www.microrna.org) and got 12 putative miRNAs for target gene NLRP3 (Figure 6A). We used qRT-PCR to detect changes in the expression of 12 miRNAs in two models of chronic liver injury induced by CCl_4 or MCDHF diet.

The hepatic expression of miR-30b-5p, miR-186-5p, miR-539-5p, and miR-216b-5p was significantly downregulated after 4 weeks of CCl_4 administration (Figure 6B). Meanwhile, the expression of miR-7a-5p, miR-30a-5p, miR-30b-5p, miR-223-3p, and miR-485-5p were significantly downregulated after 2 weeks of MCDHF diet

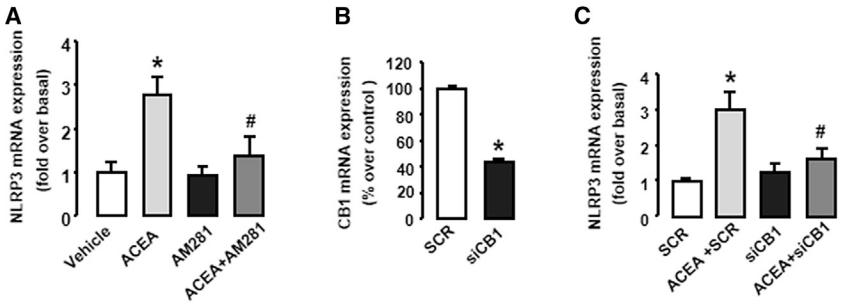

Figure 4. The NLRP3 Expression Was Mediated by CB1 Activation in Macrophages

BMMs were treated with 1 μmol/L CB1 agonist ACEA for 6 h to examine NLRP3 mRNA and 12 h to detect IL-1β protein, with the pre-treatment of 10 μmol/L CB1 antagonist AM281. (A) NLRP3 mRNA expression was examined by qRT-PCR in ACEA-treated BMMs with or without AM281. (B) Transfection efficiency of CB1 siRNA. (C) NLRP3 mRNA expression in ACEA-treated BMMs with or without CB1 siRNA. Data are presented as the mean ± SEM. n = 6 per group. *p < 0.05 versus control. #p < 0.05 versus ACEA-treated alone.

feeding compared with the control group (Figure 6C). Based on the fact that only miR-30b-5p expression was downregulated in both liver injury models, we focused on miR-30b-5p in future studies and investigated whether miR-30b-5p was involved in the regulation of NLRP3 mRNA expression by CB1. We further analyzed the correlation between hepatic miR-30b-5p level and NLRP3 mRNA expression. A straight-line fit was obtained between miR-30b-5p and NLRP3 expression, with the correlation coefficient r = −0.836 in mouse (Figure 6D).

Moreover, we tested the expression of NLRP3 and miR-30b-5p in patient liver of different etiologies, including chronic hepatitis B virus and hepatitis C virus infections, alcohol abuse, drug-induced and autoimmune liver disease, and so on and obtained a negative correlation between NLRP3 and miR-30b-5p as well (Figure 6E). These results suggested that miR-30b-5p might be able to regulate NLRP3 mRNA expression in both human and mouse inflammatory liver, independent of species and etiology. Furthermore, CB1 blockade with AM281 administration increased the hepatic level of miR-30b-5p in injured livers of CCl_4 and MCDHF mice (Figure 6F), indicating the potential role of CB1/miR-30b-5p axis in NLRP3 inflammasome.

miR-30b-5p Was Involved in CB1-Mediated NLRP3 Expression and Inflammasome Activation in Macrophages by Directly Targeting NLRP3

To investigate whether miR-30b-5p was involved in the regulation of CB1-mediated NLRP3 mRNA upregulation, we measured the expression of miR-30b-5p after CB1 activation by ACEA stimulation in BMMs, finding that miR-30b-5p expression was markedly decreased with the treatment of ACEA compared with the control group (Figure 7A). BMM cells were transfected with miR-30b-5p mimic or inhibitor to alter its expression and treated with or without CB1 agonist ACEA for 6 h. The transfected efficiency of miR-30b-5p mimic (Figures 7B, left) and inhibitor (Figures 7B, right) was verified by qRT-PCR analysis. Overexpression of miR-30b-5p with its mimic inhibited the mRNA expression of NLRP3 induced by ACEA, while miR-30b-5p inhibition by its inhibitor resulted in the upregulation of NLRP3 mRNA level (Figure 7C). Furthermore, the increased protein levels of NLRP3 and NLRP3 inflammasome activation product IL-1β induced by ACEA were suppressed after the transfection of miR-30b-5p mimic, and on the contrary, transfection of miR-30b-5p inhibitor promoted the protein expression of NLRP3 and IL-1β in BMMs (Figure 7D). To confirm the binding of miR-30b-5p with NLRP3, we transfected cells with biotinylated miR-30b-5p mimic, incubated them with streptavidin-coupled beads, and then conducted qRT-PCR to measure the amount of bound RNAs. The biotin-avidin pull-down assay uncovered that NLRP3 could be pulled down by wild-type bio-miR-30b-5p, whereas it could not be pulled down by the bio-control (Figure 7E), indicating the direct binding of miR-30b-5p with NLRP3 mRNA. Luciferase reporter assays were used to further validate that NLRP3 was a direct target of miR-30b-5p. Luciferase reporter genes were constructed using the NLRP3 3′ UTR and the mutant counterpart at the miR-30b-5p-binding regions, and miR-30b-5p mimic was co-transfected into the cells. Overexpression of miR-30b-5p significantly inhibited the luciferase activity of NLRP3 with the wild-type 3′ UTR, but not with mutant 3′ UTR (Figure 7F). Altogether, these results provided clear evidence that NLRP3 was a direct and functional downstream target of miR-30b-5p, and miR-30b-5p was involved in CB1-mediated activation of NLRP3 inflammasome in macrophages by targeting NLRP3 mRNA.

miR-30b-5p Targeted NLRP3 and Attenuated Liver Inflammation *In Vivo*

Finally, we investigated the regulation of miR-30b-5p on NLRP3 expression and liver inflammation *in vivo*, through the injection of miR-30b-5p agomir into MCDHF mice. The hepatic expression of miR-30b-5p was first examined by qRT-PCR, verifying the effectiveness and specificity of miR-30b-5p agomir *in vivo* (Figure 8A). The NLRP3 mRNA (Figure 8B) and protein levels (Figure 8C) were markedly attenuated after the injection of miR-30b-5p agomir in MCDHF mice. In line with NLRP3 expression, IL-1β protein expression also presented a significant drop in the presence of miR-30b-5p agomir in MCDHF mice (Figure 8D). Liver histology was evaluated by H&E staining (Figure 9A) and quantified by digital image analysis (Figure 9B). H&E-stained sections showed a decrease in liver injury following miR-30b-5p agomir administration in MCDHF mice (Figure 9A). Moreover, the area of inflammation displayed a partial decrease of liver inflammation after the injection of miR-30b-5p agomir in the injured liver, which was not like the total blockage of CB1 agonist AM281 (Figure 9B). Taken together, these results validated that miR-30b-5p targeted NLRP3 and partially attenuated liver inflammation *in vivo*.

DISCUSSION

Here we characterize the vital role of CB1 and miR-30b-5p in regulating NLRP3 expression and NLRP3 inflammasome activation in

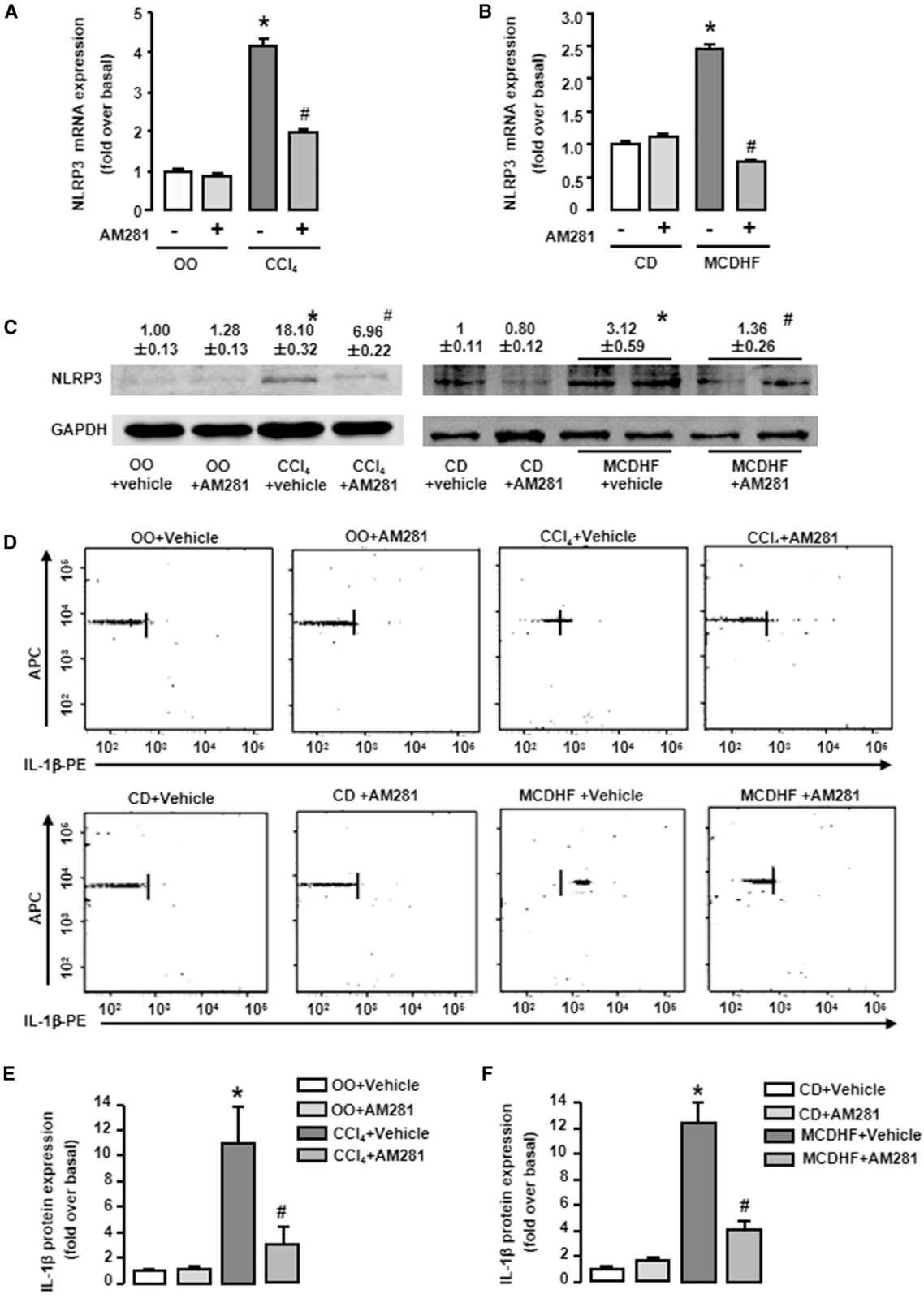

(legend on next page)

macrophages during liver inflammation injury. Our work provides several new findings as follows: (1) CB1 expression is increased in injured liver and isolated liver macrophages during chronic liver injury, positively correlated with NLRP3 expression; (2) CB1 activation promotes NLRP3 expression and NLRP3 inflammasome activation in macrophages; (3) miR-30b-5p, screened by the intersection of bioinformatics databases and downregulated miRNAs in the injured liver, participates in CB1-mediated activation of NLRP3 inflammasome in macrophages by directly targeting NLRP3; (4) CB1 blockade increases the hepatic level of miR-30b-5p, reduces NLRP3 expression, activation of NLRP3 inflammasome, and liver inflammation *in vivo*; and (5) miR-30b-5p targets NLRP3 and attenuates liver inflammation *in vivo*.

Modulation of ESC has been considered to be an important therapeutic target in inflammatory and autoimmune diseases.[32,33] For example, WWL70, inhibitor of 2-AG hydrolytic enzyme, inhibited experimental autoimmune encephalomyelitis-induced symptoms and reduced inducible nitric oxide synthase (iNOS), cyclooxygenase-2 (COX-2), tumor necrosis factor (TNF), and IL-1β expression, as well as nuclear factor κB (NF-κB) phosphorylation in the central nervous system.[34] CB1 signaling contributed to insulin resistance in both type 1 and 2 diabetes mellitus, and CB1 blockade inhibited hyperglycemia and controlled obesity in mice and cannabis users.[35,36] Importantly, CB1 antagonist contributed to the beneficial effects on lipid metabolism, anti-inflammatory and anti-fibrogenic properties in various aspects of liver pathophysiology.[37] CB1 inactivation in fatty acid amide hydrolase-deficient mice suppressed hepatocarcinogenesis through decreased hepatocyte proliferation and liver fibrosis.[38] Our previous studies had also proved that CB1 inhibition resulted in the reduced cytokine expression and phagocytosis of macrophages in CCl_4-induced chronic liver injury.[27–29] Here we further characterized the role of CB1 in macrophage NLRP3 inflammasome in the injured livers of two different mouse models and patients with chronic liver disease of different etiologies, demonstrating that CB1 activation mediated the upregulation of NLRP3 expression and activation of NLRP3 inflammasome, and CB1 blockade by its antagonist AM281 *in vivo* reversed NLRP3 inflammasome activation and liver inflammation. These data may further provide a rationale for the use of CB1 antagonists, especially peripherally restricted CB1 antagonists in liver inflammatory disease. There were also studies reporting the anti-inflammatory action of CB1 activation.[39,40] For instance, activation of cannabinoid receptors by JZL184 decreased immune cell influx and cytokine production and alleviated lung pathology.[39] A possible explanation for this discrepancy might be different cell types in vastly different micro-environments for a variety of diseases. Moreover, due to the weak affinity between ACEA and CB2, further study will be needed to explore the effect of CB2 on NLPR3 inflammasome and the specific contribution of CB1 versus CB2 to NLRP3 inflammasome activation in our cell and mouse models.

Nucleic acid-based therapy has shown great promise in a variety of diseases.[41] Especially miRNA and siRNA exert their function in the cytoplasm, thereby being more efficient in hard-to-transfect cells, such as primary cells.[42–44] The aberrant expression of specific miRNAs has been implicated in the development and progression of diverse diseases.[31,45] Genetic replacement or knockdown of target miRNAs by chemical molecules, referred to as miRNA mimic or inhibitor, has been used to reverse their abnormal expression and adverse biological effects. Here we used miR-30b-5p mimic and inhibitor *in vitro* to investigate the direct negative regulation of miR-30b-5p on NLPR3 expression. In addition to NLRP3, miR-30b-5p could also inhibit other target mRNAs. For instance, miR-30b-5p overexpression led to downregulation of MBNL1 in vascular smooth muscle cell and influenced its proliferation and differentiation in patients with coronary atherosclerosis.[46] Inhibition of miR-30b-5p protected cardiomyocytes against hypoxia-induced injury by targeting Aven.[47] miR-30b-5p directly targeted the Scn8a 3′ UTR and alleviated the oxaliplatin-induced chronic neuropathic pain by the negative regulation of the voltage-gated sodium channel $Na_v1.6$ expression in DRG neurons of rats.[48] What is more, miR-30b-5p agomir (mimic *in vivo*) was injected into liver injury mice via tail vein injection in the present study. Administration of miR-30b-5p agomir strikingly attenuated liver inflammation in MCDHF mice, as demonstrated by the decreased IL-1β expression, less hepatic steatosis, lobular inflammation, and hepatocyte ballooning, highlighting the miRNA-based treatment for liver inflammatory diseases. Here we injected 5 nM miR-30b-5p agomir into day 14 MCDHF mice and observed the therapeutic effect of miR-30b-5p on liver inflammation, and further studies will be needed to verify the anti-inflammatory effect of miR-30b-5p with different concentrations in multiple liver injury models and patients with liver disease.

Here we displayed the increased expression of NLRP3 and the negative correlation between the expression of NLRP3 and miR-30b-5p in both mouse and human injured liver. Mouse liver injury was induced by CCl_4 injection or feeding with an MCDHF diet, which were two typical liver injury models.[49,50] Human liver samples were obtained from patients with chronic liver disease of different etiologies, including chronic HBV, HCV infections, alcoholic, cryptogenic, cholestatic, drug-induced, and autoimmune liver disease. Thus, our results revealed the universal regulation of miR-30b-5p on NLRP3 inflammasome regardless of species and the etiology of liver diseases, suggesting the great potential of miR-30b-5p/NLRP3-based therapies for liver diseases. NLRP3 CreZ knockin mice exhibited growth

Figure 5. The Blockade of CB1 on NLRP3 Expression and NLRP3 Inflammasome Activation *In Vivo*

CB1 antagonist AM281 (2.5 mg/kg BW) was injected intraperitoneally to CCl_4-treated mice for 28 days or MCDHF mice for 14 days. (A and B) NLRP3 expression in the liver of CCl_4 (A) and MCDHF (B) with or without AM281 administration. (C) NLRP3 protein expression was examined by western blot in the injured liver of CCl_4 and MCDHF mice. (D) Hepatic IL-1β level was examined by CBA in the CCl_4 and MCDHF mice. (E) IL-1β protein level in the liver of CCl_4 mice. (F) IL-1β protein level in the liver of MCDHF mice. Data are presented as the mean ± SEM. n = 6 per group. *$p < 0.05$ versus control. #$p < 0.05$ versus CCl_4- or MCDHF-treated alone. OO, olive oil; CCl_4, carbon tetrachloride; CD, control diet; MCDHF, methionine-choline-deficient and high fat.

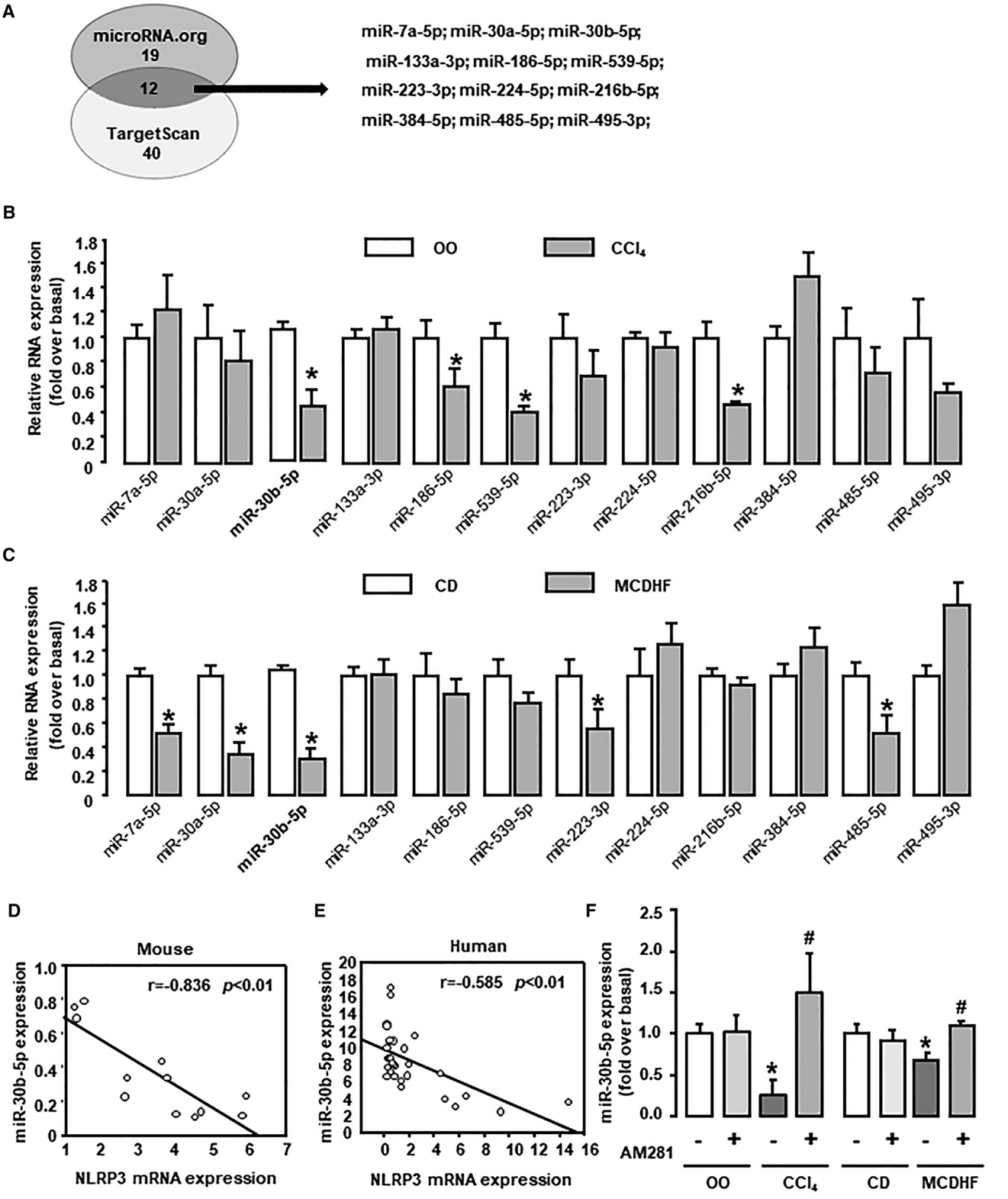

(legend on next page)

retardation and significantly lower body weight by post birth day 5 and usually died at 2–3 weeks with higher liver weight/body weight. Further studies will be needed to explore the role of NLRP3 in normal tissues, especially on cell survival.

In conclusion, we reveal the critical role CB1/miR-30b-5p/NLRP3 axis in chronic liver inflammation and fibrogenesis. miR-30b-5p participates in CB1-mediated activation of NLRP3 inflammasome in macrophages by directly targeting NLRP3 3′ UTR and downregulating its mRNA expression. What's more, administration of CB1 inhibitor AM281 or miR-30b-5p agomir reduces NLRP3 expression and activation of NLRP3 inflammasome and attenuates liver inflammation *in vivo*, which indicates CB1/miR-30b-5p/NLRP3 signaling as target for treatment of liver disease.

MATERIALS AND METHODS

Mouse Models

To induce CCl_4-induced liver injury model, mice received intraperitoneal injections of 1 μL per gram body weight (BW) of a CCl_4/olive oil (OO) mixture (1:9 v/v) twice per week, and were sacrificed at day 2, 3, 7, 14, or 28. The intraperitoneal injection of AM281 (2.5 mg/kg BW) was performed at 4 h before CCl_4 administration for 28 days. Another liver injury model was induced by MCDHF diet (A06071309, Research Diet, NJ, USA) feeding. Mice were sacrificed at day 2, 3, 7, 14, or 28. The intraperitoneal injection of AM281 (2.5 mg/kg BW) was performed twice per week in day 14 MCDHF mice. miR-30b-5p agomir (Guangzhou RiboBio, CHN) was delivered *in vivo* using a "hydrodynamic transfection method," by which 5 nM miR-30b-5p agomir was rapidly injected into the tail vein twice per week in day 14 MCDHF mice. Control mice were injected with an equal volume of control agomir dissolved in PBS. Liver tissue and blood samples were collected. All animal work was conformed to the Ethics Committee of Capital Medical University and in accordance with the approved guidelines (approval number: AEEI-2014-131).

Isolation of Mouse Liver Macrophages

Liver macrophages were isolated from mice. Anesthetized and heparinized mice were subjected to a midline laparotomy and cannulation of the portal vein followed by liver perfusion with an EGTA-chelating perfusion buffer. After perfusion with 0.4% collagenase buffer, livers were torn and cells dispersed in saline; macrophages were separated using low-speed centrifugation and 70%/30% percoll density gradient centrifugation (middle layer). The identification of macrophages was assessed using FACS analysis of F4/80 expression.

Isolation and Culture of BMMs

Cells were obtained from the tibia and femur bone marrow of ICR (Institute of Cancer Research) mice. Bone marrow cells were extracted from the tibias and femurs by flushing with culture medium using a 25G needle. The cells were then passed through a 70-mm nylon mesh and were washed three times with PBS containing 2% FBS. Bone marrow cells were grown in culture dishes for 7 days in the presence of L929-conditioned medium. BMMs were treated with 1 μmol/L special CB1 agonist ACEA (TOCRIS/R&D, MN, USA) for 6 h to examine NLRP3 mRNA and 12 h to detect IL-1β protein. 10 μM CB1 antagonist AM281 (TOCRIS/R&D, MN, USA) was pre-treated 1 h before the stimulation of ACEA.

Human Liver Specimen

Human fibrotic samples (fibrosis stage: F2–4) were obtained from livers of 30 patients undergoing liver biopsy (18 men, 12 women; mean age, 58 years; range, 25–76 years). Fibrosis was consecutive to chronic HBV (n = 10), HCV (n = 5), alcoholic (n = 5), cryptogenic (n = 3), cholestatic (n = 3), drug-induced (n = 1), and autoimmune (n = 3) liver disease. Normal liver samples were collected from 8 patients undergoing hepatic resection for hepatic hemangioma. All subjects gave their informed consent for inclusion before they participated in the study. The study was conducted in accordance with the Declaration of Helsinki, and the protocol was approved by the Ethics Committee of Beijing Shijitan Hospital, Capital Medical University, Beijing, China (project identification code: 2018EC-1).

FACS

Non-parenchymal cells of mouse liver were isolated as described previously.[51] APC-F4/80 antibody (eBioscience, San Diego, CA, USA) and its isotype-matched negative control were added to the non-parenchymal cells, respectively. After 15 min incubation in the dark, the cells were washed with PBS and subjected to FACS, which was performed on a FACSAria and analyzed with FACS Diva 4.1 (BD, Biosciences, NJ, USA).

qRT-PCR

Extraction of total RNA from mice liver frozen specimen and qRT-PCR were performed. Primers were as follows: 18S rRNA: sense, 5′-GTA ACC CGT TGA ACC CCA TT-3′; antisense, 5′-CCA TCC AAT CGG TAG TAG CG-3′. mouse NLRP-3: sense, 5′-ATT ACC CGC CCG AGA AAG G-3′; antisense, 5′-TCG CAG CAA AGA TCC ACA CAG-3′. Mouse CB1: sense, 5′-GGC GGT GGC CGA TCT C-3′; antisense, 5′-CGG TAA CCC CAC CCA GTT T-3′. Human NLRP-3: sense, 5′-GAT CTT CGC TGC GAT CAA CAG-3′; antisense, 5′-CGT GCA TTA TCT GAA CCC CAC-3′.

Figure 6. miR-30b-5p Targeting NLRP3 Was Screened

(A) The screen of miRNAs targeting NLRP3. (B) The miRNA expression was examined by qRT-PCR in the fibrotic liver induced by CCl_4. (C) The miRNA expression in the fibrotic liver induced by MCDHF. (D) The correlation between NLRP3 and miR-30b-5p in mouse liver tissue. (E) The correlation between NLRP3 and miR-30b-5p in human liver tissue. (F) miR-30b-5p expression was examined by qRT-PCR in the liver of CCl_4 and MCDHF mice with or without AM281 administration. Data are presented as the mean ± SEM. n = 6 per group. *$p < 0.05$ versus control. #$p < 0.05$ versus CCl_4- or MCDHF-treated alone. OO, olive oil; CCl_4, carbon tetrachloride; CD, control diet; MCDHF, methionine-choline-deficient and high fat.

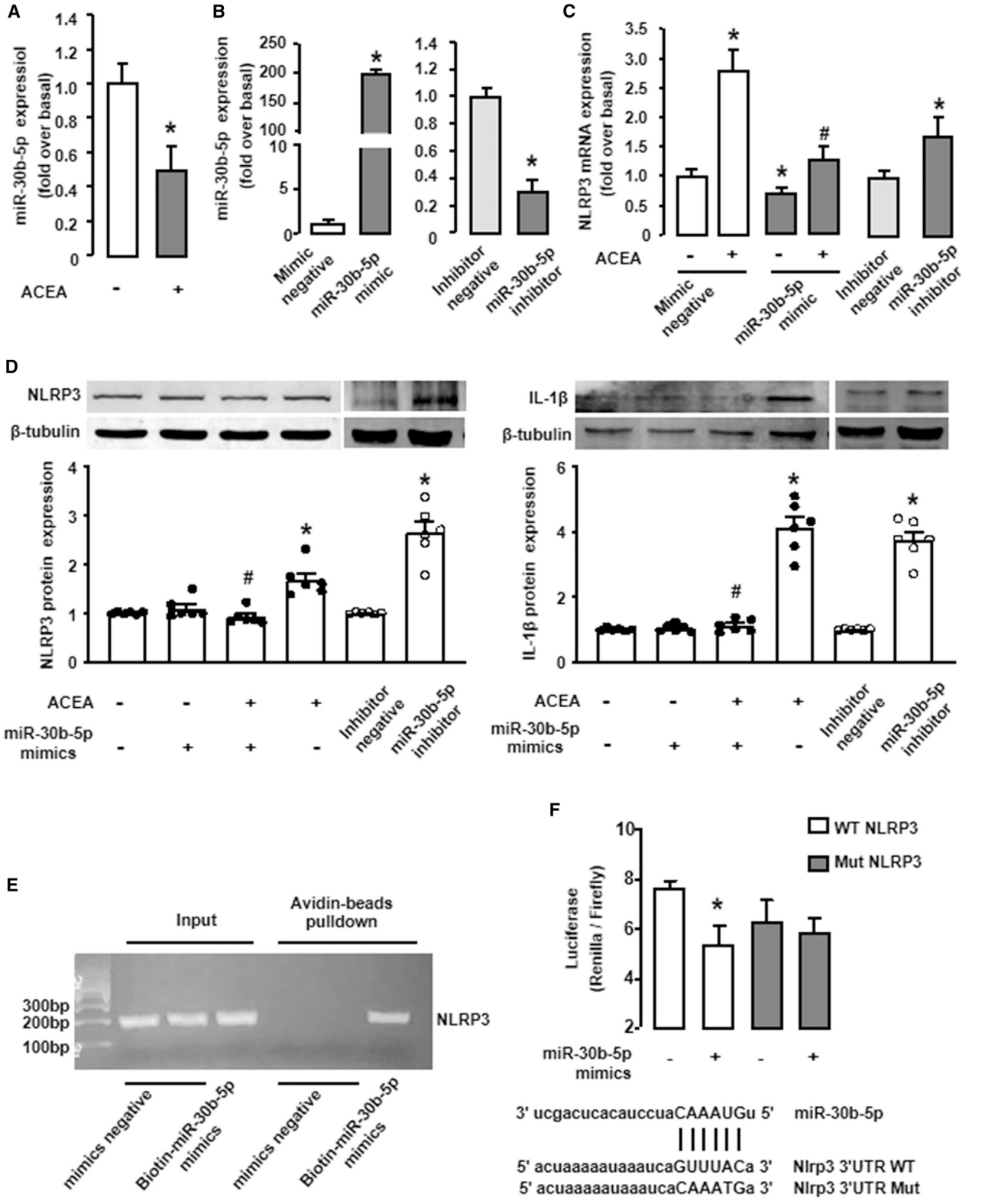

(legend on next page)

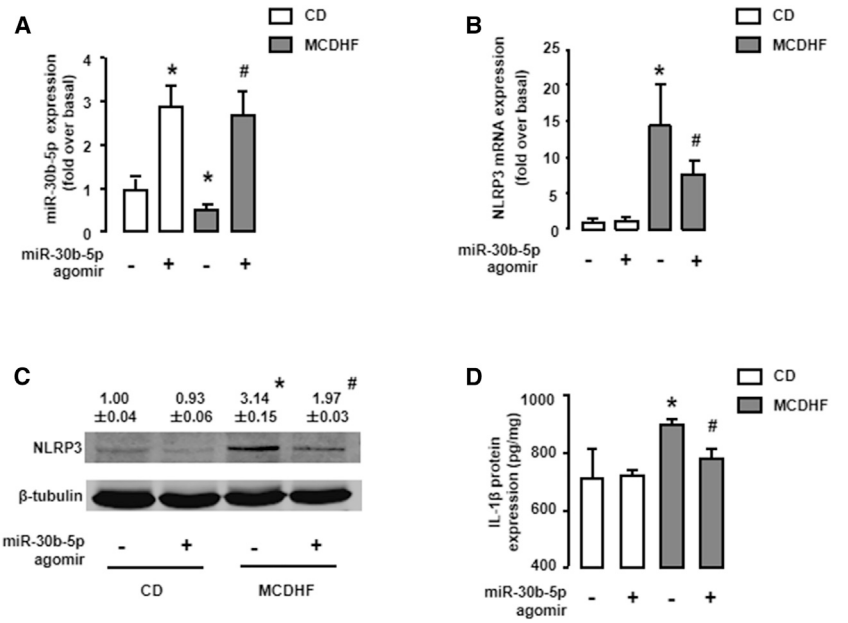

Figure 8. The Effect of miR-30b-5p on NLRP3 Expression and Inflammasome Activation *In Vivo*

5 nM miR-30b-5p agomir (mimic *in vivo*) or agomir negative control was injected into the tail vein twice per week in day 14 MCDHF mice. "+" represented injection of miR-30b-5p agomir, "–" represented injection of agomir negative control. (A) Transfection efficiency of miR-30b-5p agomir in the liver of MCDHF mice. (B) NLRP3 mRNA levels in liver tissue were measured by qRT-PCR with or without miR-30b-5p agomir injection in MCDHF mice. (C) NLRP3 protein levels in liver tissue were measured by western blot. (D) IL-1β protein expression was examined by ELISA with or without miR-30b-5p agomir injection in MCDHF mice. Data are presented as the mean ± SEM. n = 6 per group. *p < 0.05 versus control. #p < 0.05 versus MCDHF-treated alone. CD, control diet; MCDHF, methionine-choline-deficient and high fat.

Western Blot

Western blot for NLRP3 and IL-1β was performed with 50 μg of protein extract using monoclonal antibodies to NLRP3 (1:2,000, Adipogen, CA, USA), IL-1β (1:2,000, CST, MA, USA) and the appropriate IRDyeTM 800-conjugated secondary antibody (1:10,000). Signals were detected using the Odyssey Imaging System (LI-COR Biosciences, Lincoln, NE, USA) and analyzed with Odyssey software. Results were normalized relative to GAPDH (1:1,000, CST, MA, USA) or β-tubulin (1:2,000, Transgen Biotech, CHN) expression to correct for variations in protein loading and transfer.

Measurement of Cytokines and Chemokines by Cytometric Bead Array (CBA)

BMMs (500,000 cells) were lysed in 40 mL lysis buffer. IL-1β in homogenates was detected using CBA mouse IL-1β Flex Set (catalog number 558266, BD Biosciences, NJ, USA) and then analyzed by FACS.

Measurement of IL-1β by ELISA

The concentration of IL-1β in liver tissue was measured by IL-1β ELISA kit (DAKEWE, CHN) according to the manufacturer's instructions. A standard curve was created and results were normalized to the protein content of the sample.

RNA Interference and Transfection

The siRNA targeting CB1 was purchased from Invitrogen (Thermo Fisher Scientific, PA, USA). miR-30b-5p mimic or inhibitor was designed and synthesized by RiboBio (Guangzhou, CHN). The sequences of miR-30b-5p mimic, sense, 5′-UGUAAACAUCC UACACUCAGCU-3′; anti-sense, 5′-AGCUGAGUGUAGGAU GUUUACA-3′. The sequences of miR-30b-5p inhibitor, 5′-AGCU GAGUGUAGGAUGUUUACA-3′. BMMs were transfected with 40 nM CB1 siRNA, miR-30b-5p mimic or inhibitor, and correlated negative controls using Lipofectamine RNAiMAX (Invitrogen, Carlsbad, CA, USA) for 6–8 h as recommended by the manufacturer. After 24 or 48 h, cells were collected to perform further experiments.

Pull-Down Assay

Biotinylated miR-30b-5p mimics and negative control mimics (Beijing AuGCT Biotechnology, CHN) were respectively transfected into BMMs. Cells lysate were then incubated with streptavidin-coupled magnetic beads (Dynabeads M-280 Streptavidin, Thermo Fisher Scientific, Waltham, MA, USA) for purifying target RNA in accordance with the manufacturer's instructions. The RNA amplification products quantified and analyzed by qRT-PCR were used for DNA agarose gel electrophoresis.

Figure 7. The Regulation of miR-30b-5p on NLRP3 Expression and NLRP3 Inflammasome Activation in BMMs

(A) miR-30b-5p expression in CB1 agonist ACEA-treated BMMs. (B) miR-30b-5p expression in BMMs transfected with miR-30b-5p mimic or inhibitor. (C) NLRP3 mRNA expression was examined by qRT-PCR with or without miR-30b-5p mimic or inhibitor transfection in ACEA-treated BMMs. (D) NLRP3 protein expression was examined by western blot with miR-30b-5p mimic or inhibitor transfection in BMMs. (E) Binding of miR-30b-5p with NLRP3 mRNA by biotin-avidin pull-down assay. (F) Luciferase reporter assay was performed to demonstrate NLRP3 was a target of miR-30b-5p. Data are presented as the mean ± SEM. n = 6 per group. *p < 0.05 versus control. #p < 0.05 versus ACEA-treated alone.

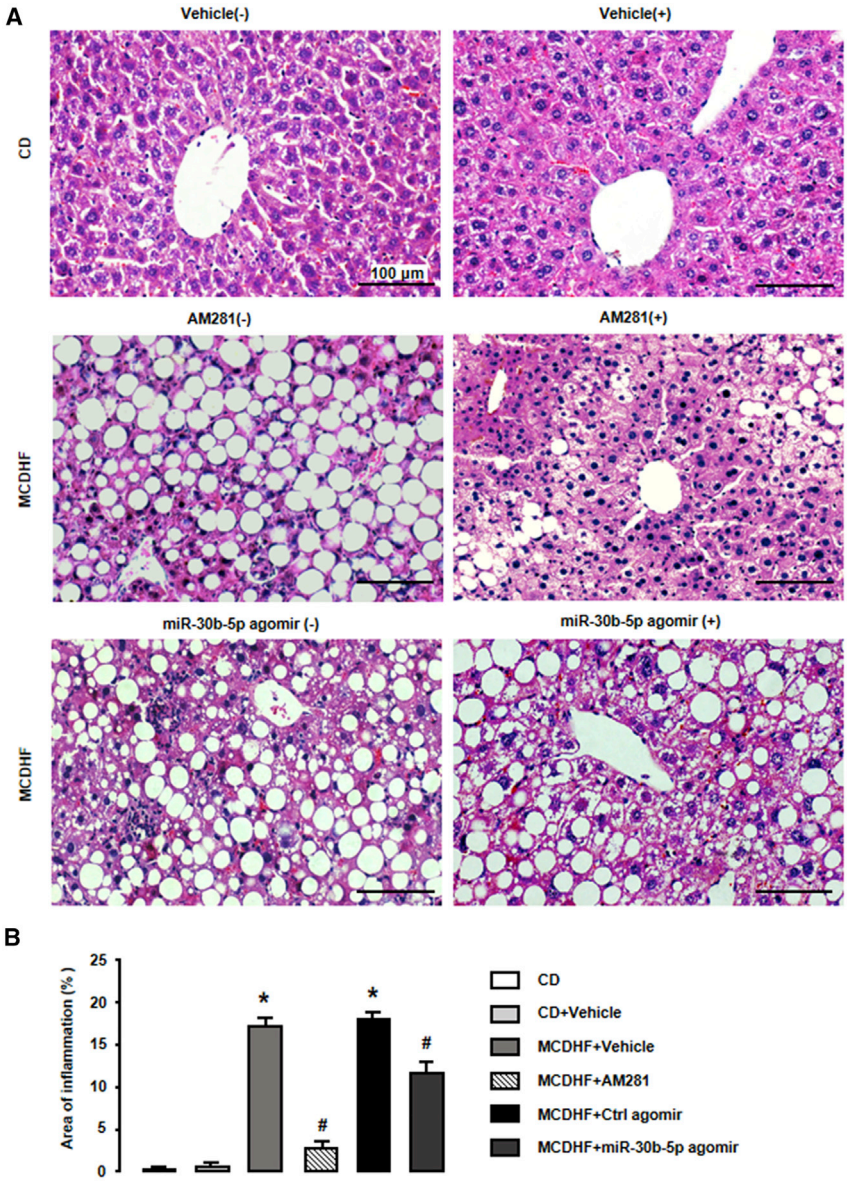

Figure 9. The Effect of AM281 and miR-30b-5p on Liver Inflammation *In Vivo*

(A) Representative H&E-staining liver sections in MCDHF mice with the injection of CB1 antagonist AM281 or miR-30b-5p agomir (mimic *in vivo*). (B) The area of inflammation was quantified by digital image analysis. Data are presented as the mean ± SEM. n = 6 per group. *p < 0.05 versus control. #p < 0.05 versus MCDHF-treated alone. CD, control diet; MCDHF, methionine-choline-deficient and high fat.

Luciferase Reporter Assays

BMMs were seeded in 96-well plates 24 h prior to transfection. Subsequently, the cells were transiently co-transfected with 1 ng/μL wild-type or mutant reporter plasmid (Guangzhou RiboBio, CHN) and 50 nM miR-30b-5p mimic or miR-control using Lipofectamine 2000. Firefly and Renilla luciferase activities were measured 48 h subsequent to transfection using the Dual Luciferase Assay (Promega, Madison, WI, USA), according to the manufacturer's protocol. Renilla luciferase activity was normalized to Firefly, and the value of Renilla luciferase activity/Firefly luciferase activity was analyzed.

Immunofluorescence Staining

Liver samples were fixed in 4% paraformaldehyde and embedded in Tissue Tek OCT compound. 5 μm of frozen section were used for immunofluorescence. Liver sections were blocked with 2% BSA, and then incubated with NLRP3 (1:400, Adipogen, CA, USA) or F4/80 antibody (1:100, Santa Cruz Biotechnology, CA, USA), Cy3-AffiniPure goat anti-mouse immunoglobulin G (IgG) or fluorescein isothiocyanate (FITC)-AffiniPure goat anti-rat IgG (1:100, Jackson Immunoresearch, West Grove, PA, USA) was used as secondary antibodies. The samples were covered with Vectashield mounting medium containing DAPI (4,6-diamino-2-phenylindole) and observed under confocal microscope (LSM510, Carl Zeiss MicroImaging GmbH, Germany).

Histology Analysis

Liver tissues were fixed in 4% paraformaldehyde for 24 h and embedded in paraffin. Liver tissue sections (5 μm) were stained with H&E for assessment of liver inflammation and injury. The inflammatory response was quantified by measuring the inflammatory area using ImageJ software. We measured 15 randomly selected areas per sample and calculated the mean value of the percentage of inflammatory area accounting for total area.

Data and Statistical Analysis

The results are expressed as mean ± standard error of the mean (SEM). Statistical significance was assessed by Student's t test or one-way analysis of variance (ANOVA) for analysis of variance with post hoc Tukey's multiple comparison tests when appropriate. Correlation coefficients were calculated by Pearson test. $p < 0.05$ was considered to be significant. All results were verified in at least three independent experiments.

AUTHOR CONTRIBUTIONS

Study concept and design (L.L.), acquisition of data (Le Yang, L.T., Z.Z., X.Z., X.J., F.L., C.D.), analysis and interpretation of data (Le Yang, L.T., Z.Z., L.H., X.Z., N.C., and Lin Yang), drafting of the manuscript (Le Yang and L.L.), study supervision (L.L.).

CONFLICTS OF INTEREST

The authors declare no competing interests.

ACKNOWLEDGMENTS

This work was supported by grants from the National Natural and Science Foundation of China (81670550 and 81430013).

REFERENCES

1. Awad, F., Assrawi, E., Louvrier, C., Jumeau, C., Georgin-Lavialle, S., Grateau, G., Amselem, S., Giurgea, I., and Karabina, S.A. (2018). Inflammasome biology, molecular pathology and therapeutic implications. Pharmacol. Ther. *187*, 133–149.
2. Schroder, K., and Tschopp, J. (2010). The inflammasomes. Cell *140*, 821–832.
3. Zhang, P., Cao, L., Zhou, R., Yang, X., and Wu, M. (2019). The lncRNA Neat1 promotes activation of inflammasomes in macrophages. Nat. Commun. *10*, 1495.
4. Jiang, H., He, H., Chen, Y., Huang, W., Cheng, J., Ye, J., Wang, A., Tao, J., Wang, C., Liu, Q., et al. (2017). Identification of a selective and direct NLRP3 inhibitor to treat inflammatory disorders. J. Exp. Med. *214*, 3219–3238.
5. Kumar, B., Cashman, S.M., and Kumar-Singh, R. (2018). Complement-Mediated Activation of the NLRP3 Inflammasome and Its Inhibition by AAV-Mediated Delivery of CD59 in a Model of Uveitis. Mol. Ther. *26*, 1568–1580.
6. Yang, Y., Wang, H., Kouadir, M., Song, H., and Shi, F. (2019). Recent advances in the mechanisms of NLRP3 inflammasome activation and its inhibitors. Cell Death Dis. *10*, 128.
7. Wang, X., Gao, Y., Song, J., Tang, C., Wang, M., Que, L., Liu, L., Zhu, G., Chen, Q., Yao, Y., et al. (2017). The TIR/BB-loop mimetic AS-1 prevents non-alcoholic steatohepatitis and hepatic insulin resistance by inhibiting NLRP3-ASC inflammasome activation. Br. J. Pharmacol. *174*, 1841–1856.
8. Broderick, L., De Nardo, D., Franklin, B.S., Hoffman, H.M., and Latz, E. (2015). The inflammasomes and autoinflammatory syndromes. Annu. Rev. Pathol. *10*, 395–424.
9. Lamkanfi, M., and Dixit, V.M. (2012). Inflammasomes and their roles in health and disease. Annu. Rev. Cell Dev. Biol. *28*, 137–161.
10. Li, C., Jin, Y., Wei, S., Sun, Y., Jiang, L., Zhu, Q., Farmer, D.G., Busuttil, R.W., Kupiec-Weglinski, J.W., and Ke, B. (2019). Hippo Signaling Controls NLR Family Pyrin Domain Containing 3 Activation and Governs Immunoregulation of Mesenchymal Stem Cells in Mouse Liver Injury. Hepatology *70*, 1714–1731.
11. Strowig, T., Henao-Mejia, J., Elinav, E., and Flavell, R. (2012). Inflammasomes in health and disease. Nature *481*, 278–286.
12. Vandanmagsar, B., Youm, Y.H., Ravussin, A., Galgani, J.E., Stadler, K., Mynatt, R.L., Ravussin, E., Stephens, J.M., and Dixit, V.D. (2011). The NLRP3 inflammasome instigates obesity-induced inflammation and insulin resistance. Nat. Med. *17*, 179–188.
13. Wree, A., Eguchi, A., McGeough, M.D., Pena, C.A., Johnson, C.D., Canbay, A., Hoffman, H.M., and Feldstein, A.E. (2014). NLRP3 inflammasome activation results in hepatocyte pyroptosis, liver inflammation, and fibrosis in mice. Hepatology *59*, 898–910.
14. Humphries, B., Wang, Z., and Yang, C. (2019). MicroRNA Regulation of Epigenetic Modifiers in Breast Cancer. Cancers (Basel) *11*, E897.
15. Kristensen, L.S., Andersen, M.S., Stagsted, L.V.W., Ebbesen, K.K., Hansen, T.B., and Kjems, J. (2019). The biogenesis, biology and characterization of circular RNAs. Nat. Rev. Genet. *20*, 675–691.
16. Sun, Z., Shi, K., Yang, S., Liu, J., Zhou, Q., Wang, G., Song, J., Li, Z., Zhang, Z., and Yuan, W. (2018). Effect of exosomal miRNA on cancer biology and clinical applications. Mol. Cancer *17*, 147.
17. Hu, Z., Lv, X., Chen, L., Gu, X., Qian, H., Fransisca, S., Zhang, Z., Liu, Q., and Xie, P. (2019). Protective effects of microRNA-22-3p against retinal pigment epithelial inflammatory damage by targeting NLRP3 inflammasome. J. Cell. Physiol. *234*, 18849–18857.
18. Ning, Z.W., Luo, X.Y., Wang, G.Z., Li, Y., Pan, M.X., Yang, R.Q., Ling, X.G., Huang, S., Ma, X.X., Jin, S.Y., et al. (2017). MicroRNA-21 Mediates Angiotensin II-Induced Liver Fibrosis by Activating NLRP3 Inflammasome/IL-1β Axis via Targeting Smad7 and Spry1. Antioxid. Redox Signal. *27*, 1–20.
19. Byeon, H.E., Jeon, J.Y., Kim, H.J., Kim, D.J., Lee, K.W., Kang, Y., and Han, S.J. (2017). MicroRNA-132 Negatively Regulates Palmitate-Induced NLRP3 Inflammasome Activation through FOXO3 Down-Regulation in THP-1 Cells. Nutrients *9*, E1370.
20. Song, J., Yang, S., Yin, R., Xiao, Q., Ma, A., and Pan, X. (2019). MicroRNA-181a regulates the activation of the NLRP3 inflammatory pathway by targeting MEK1 in THP-1 macrophages stimulated by ox-LDL. J. Cell. Biochem. *120*, 13640–13650.
21. Di Marzo, V. (2018). New approaches and challenges to targeting the endocannabinoid system. Nat. Rev. Drug Discov. *17*, 623–639.
22. Basavarajappa, B.S., Joshi, V., Shivakumar, M., and Subbanna, S. (2019). Distinct functions of endogenous cannabinoid system in alcohol abuse disorders. Br. J. Pharmacol. *176*, 3085–3109.
23. Guillot, A., Hamdaoui, N., Bizy, A., Zoltani, K., Souktani, R., Zafrani, E.S., Mallat, A., Lotersztajn, S., and Lafdil, F. (2014). Cannabinoid receptor 2 counteracts interleukin-17-induced immune and fibrogenic responses in mouse liver. Hepatology *59*, 296–306.
24. Grunewald, Z.I., Lee, S., Kirkland, R., Ross, M., and de La Serre, C.B. (2019). Cannabinoid receptor type-1 partially mediates metabolic endotoxemia-induced inflammation and insulin resistance. Physiol. Behav. *199*, 282–291.
25. Barutta, F., Bruno, G., Mastrocola, R., Bellini, S., and Gruden, G. (2018). The role of cannabinoid signaling in acute and chronic kidney diseases. Kidney Int. *94*, 252–258.
26. Mukhopadhyay, B., Schuebel, K., Mukhopadhyay, P., Cinar, R., Godlewski, G., Xiong, K., Mackie, K., Lizak, M., Yuan, Q., Goldman, D., and Kunos, G. (2015). Cannabinoid receptor 1 promotes hepatocellular carcinoma initiation and progression through multiple mechanisms. Hepatology *61*, 1615–1626.
27. Tian, L., Li, W., Yang, L., Chang, N., Fan, X., Ji, X., Xie, J., Yang, L., and Li, L. (2017). Cannabinoid Receptor 1 Participates in Liver Inflammation by Promoting M1 Macrophage Polarization *via* RhoA/NF-κB p65 and ERK1/2 Pathways, Respectively, in Mouse Liver Fibrogenesis. Front. Immunol. *8*, 1214.
28. Mai, P., Yang, L., Tian, L., Wang, L., Jia, S., Zhang, Y., Liu, X., Yang, L., and Li, L. (2015). Endocannabinoid System Contributes to Liver Injury and Inflammation by Activation of Bone Marrow-Derived Monocytes/Macrophages in a CB1-Dependent Manner. J. Immunol. *195*, 3390–3401.
29. Mai, P., Tian, L., Yang, L., Wang, L., Yang, L., and Li, L. (2015). Cannabinoid receptor 1 but not 2 mediates macrophage phagocytosis by G(α)i/o /RhoA/ROCK signaling pathway. J. Cell. Physiol. *230*, 1640–1650.
30. Bao, J., Sun, T., Yue, Y., and Xiong, S. (2019). Macrophage NLRP3 inflammasome activated by CVB3 capsid proteins contributes to the development of viral myocarditis. Mol. Immunol. *114*, 41–48.
31. Mulholland, E.J., Dunne, N., and McCarthy, H.O. (2017). MicroRNA as Therapeutic Targets for Chronic Wound Healing. Mol. Ther. Nucleic Acids *8*, 46–55.
32. Gonçalves, E.D., and Dutra, R.C. (2019). Cannabinoid receptors as therapeutic targets for autoimmune diseases: where do we stand? Drug Discov. Today *24*, 1845–1853.
33. Mallat, A., and Lotersztajn, S. (2016). Targeting cannabinoid receptors in hepatocellular carcinoma? Gut *65*, 1582–1583.
34. Wen, J., Ribeiro, R., Tanaka, M., and Zhang, Y. (2015). Activation of CB2 receptor is required for the therapeutic effect of ABHD6 inhibition in experimental autoimmune encephalomyelitis. Neuropharmacology *99*, 196–209.
35. Penner, E.A., Buettner, H., and Mittleman, M.A. (2013). The impact of marijuana use on glucose, insulin, and insulin resistance among US adults. Am. J. Med. *126*, 583–589.
36. Tam, J., Cinar, R., Liu, J., Godlewski, G., Wesley, D., Jourdan, T., Szanda, G., Mukhopadhyay, B., Chedester, L., Liow, J.S., et al. (2012). Peripheral cannabinoid-1 receptor inverse agonism reduces obesity by reversing leptin resistance. Cell Metab. *16*, 167–179.
37. Mallat, A., Teixeira-Clerc, F., and Lotersztajn, S. (2013). Cannabinoid signaling and liver therapeutics. J. Hepatol. *59*, 891–896.
38. Suk, K.T., Mederacke, I., Gwak, G.Y., Cho, S.W., Adeyemi, A., Friedman, R., and Schwabe, R.F. (2016). Opposite roles of cannabinoid receptors 1 and 2 in hepatocarcinogenesis. Gut *65*, 1721–1732.
39. Tahamtan, A., Tavakoli-Yaraki, M., Shadab, A., Rezaei, F., Marashi, S.M., Shokri, F., Mokhatri-Azad, T., and Salimi, V. (2018). The Role of Cannabinoid Receptor 1 in the Immunopathology of Respiratory Syncytial Virus. Viral Immunol. *31*, 292–298.
40. Mackovski, N., Liao, J., Weng, R., Wei, X., Wang, R., Chen, Z., Liu, X., Yu, Y., Meyer, B.J., Xia, Y., et al. (2016). Reversal effect of simvastatin on the decrease in cannabinoid receptor 1 density in 6-hydroxydopamine lesioned rat brains. Life Sci. *155*, 123–132.

41. Wang, P., Perche, F., Logeart-Avramoglou, D., and Pichon, C. (2019). RNA-based therapy for osteogenesis. Int. J. Pharm. *569*, 118594.

42. Yan, B., Wang, H., Tan, Y., and Fu, W. (2019). microRNAs in Cardiovascular Disease: Small Molecules but Big Roles. Curr. Top. Med. Chem. *19*, 1918–1947.

43. Orso, F., Quirico, L., Dettori, D., Coppo, R., Virga, F., Ferreira, L.C., Paoletti, C., Baruffaldi, D., Penna, E., and Taverna, D. (2019). Role of miRNAs in tumor and endothelial cell interactions during tumor progression. Semin. Cancer Biol. *60*, 214–224.

44. Chakraborty, C., Sharma, A.R., Sharma, G., Doss, C.G.P., and Lee, S.S. (2017). Therapeutic miRNA and siRNA: Moving from Bench to Clinic as Next Generation Medicine. Mol. Ther. Nucleic Acids *8*, 132–143.

45. Giordano, S., and Columbano, A. (2013). MicroRNAs: new tools for diagnosis, prognosis, and therapy in hepatocellular carcinoma? Hepatology *57*, 840–847.

46. Woo, C.C., Liu, W., Lin, X.Y., Dorajoo, R., Lee, K.W., Richards, A.M., Lee, C.N., Wongsurawat, T., Nookaew, I., and Sorokin, V. (2019). The interaction between *30b-5p* miRNA and *MBNL1* mRNA is involved in vascular smooth muscle cell differentiation in patients with coronary atherosclerosis. Int. J. Mol. Sci. *21*, E11.

47. Zhang, L., and Jia, X. (2019). Down-regulation of miR-30b-5p protects cardiomyocytes against hypoxia-induced injury by targeting Aven. Cell. Mol. Biol. Lett. *24*, 61.

48. Li, L., Shao, J., Wang, J., Liu, Y., Zhang, Y., Zhang, M., Zhang, J., Ren, X., Su, S., Li, Y., et al. (2019). MiR-30b-5p attenuates oxaliplatin-induced peripheral neuropathic pain through the voltage-gated sodium channel $Na_v1.6$ in rats. Neuropharmacology *153*, 111–120.

49. Yang, L., Dong, C., Yang, J., Yang, L., Chang, N., Qi, C., and Li, L. (2019). MicroRNA-26b-5p Inhibits Mouse Liver Fibrogenesis and Angiogenesis by Targeting PDGF Receptor-Beta. Mol. Ther. Nucleic Acids *16*, 206–217.

50. Li, C., Kong, Y., Wang, H., Wang, S., Yu, H., Liu, X., Yang, L., Jiang, X., Li, L., and Li, L. (2009). Homing of bone marrow mesenchymal stem cells mediated by sphingosine 1-phosphate contributes to liver fibrosis. J. Hepatol. *50*, 1174–1183.

51. Han, Z., Zhu, T., Liu, X., Li, C., Yue, S., Liu, X., Yang, L., Yang, L., and Li, L. (2012). 15-deoxy-Δ12,14 -prostaglandin J2 reduces recruitment of bone marrow-derived monocyte/macrophages in chronic liver injury in mice. Hepatology *56*, 350–360.